

# The recurrent nuclear activity of Fornax A and its interaction with the cold gas

F. M. Maccagni<sup>1</sup>, P. Serra<sup>1</sup>, M. Murgia<sup>1</sup>, F. Govoni<sup>1</sup>, K. Morokuma-Matsui<sup>2</sup>, D. Kleiner<sup>1</sup> †

<sup>1</sup>INAF – Osservatorio Astronomico di Cagliari, via della Scienza 5, 09047, Selargius (CA), Italy  
email: FILIPPO.MACCAGNI@INAF.IT

<sup>2</sup>Institute of Astronomy, Graduate School of Science, The University of Tokyo, 2-21-1 Osawa, Mitaka, Tokyo 181-0015, Japan

**Abstract.** Sensitive (noise  $\sim 16 \mu\text{Jy beam}^{-1}$ ), high-resolution ( $\sim 10''$ ) MeerKAT observations of Fornax A show that its giant lobes have a double-shell morphology, where dense filaments are embedded in a diffuse and extended cocoon, while the central radio jets are confined within the host galaxy. The spectral radio properties of the lobes and jets of Fornax A reveal that its nuclear activity is rapidly flickering. Multiple episodes of nuclear activity must have formed the radio lobes, for which the last stopped 12 Myr ago. More recently ( $\sim 3$  Myr ago), a less powerful and short ( $\lesssim 1$  Myr) phase of nuclear activity generated the central jets. The distribution and kinematics of the neutral and molecular gas in the centre give insights on the interaction between the recurrent nuclear activity and the surrounding interstellar medium.

**Keywords.** galaxies: individual: (Fornax A, NGC 1316), galaxies: active, radio continuum: galaxies, galaxies: jets, radiation mechanisms: non-thermal.

---

## 1. Introduction

The energy released by Active Galactic Nuclei (AGNs) into the surrounding interstellar medium (ISM) through radiation and/or relativistic jets of radio plasma can drastically change the fate of its host galaxy by removing or displacing the gas in the galaxy and preventing it from cooling to form new stars (e.g. Fabian 2012). This mechanism is commonly referred to as ‘AGN feedback’. Numerical simulations of galaxy evolution indicate that only multiple phases of nuclear activity, and therefore recurring episodes of AGN feedback, may prevent the hot circumgalactic gas from cooling back onto the galaxy, and explain the rapid quenching of star formation in early-type galaxies (Werner et al. 2019).

The radio emission of AGNs allows us to measure the duty cycle of the nuclear activity. In particular, the steepening of the radio spectrum is often interpreted as radiative ageing of the electron population in the relativistic plasma (e.g., Murgia et al. 1999, Harwood et al. 2013, Kolokythas et al. 2015).

In this proceeding, we summarize the study of the radio spectrum of the nearby ( $D_L \sim 20$  Mpc) radio galaxy Fornax A to determine the timescale and the duty cycle of its nuclear activity. This analysis is shown in detail in Maccagni et al. (2020).

Fornax A is one of the most fascinating radio sources in the local Universe because of its filamentary extended radio lobes ( $\sim 1.1^\circ$ , Fomalont et al. 1989). The MeerKAT (Jonas et al. 2016) observation (Fig. 1) at 1.03 GHz shows that the lobes are embedded in a diffuse cocoon, with a ‘bridge’ of synchrotron emission connecting them. In the centre, two radio jets are confined within the host galaxy ( $r \lesssim 6$  kpc) and exhibit an s-shaped

† This project has received funding from the European Research Council (ERC) under the European Unions Horizon 2020 research and innovation programme (grant agreement no. 679627).

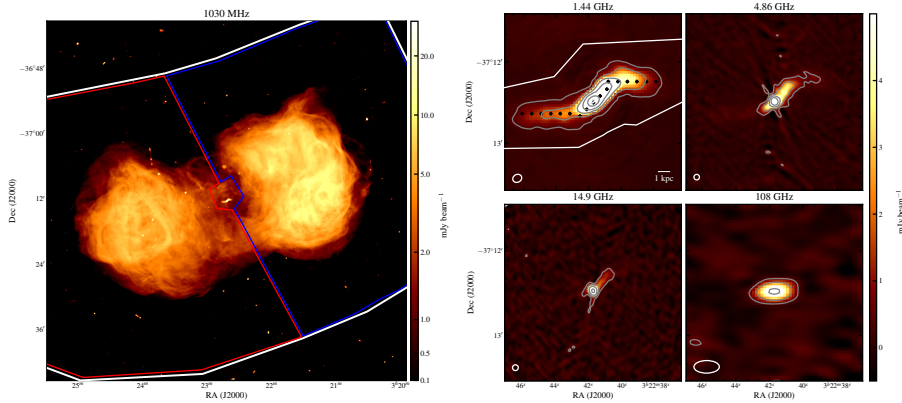


**Figure 1.** *Left panel:* Fornax A seen by MeerKAT at 1.03 GHz. The red and blue contours mark the region where we measure flux density of the east and west lobes, respectively. The synthesised beam of the image is  $11.2'' \times 9.1''$ . *Right panel:* Central emission of Fornax A seen at 1.44 GHz by MeerKAT (*top left*), at 4.86 GHz (*top right*), 14.9 GHz (*bottom left*) by the VLA and at 108 GHz (*bottom right*) by ALMA. The PSF of the images is shown in white. (Maccagni et al. 2020)

morphology. Most of the radio emission is produced in the extended lobes. At 1.4 GHz, their total flux density is 121 Jy while that of the jets is  $\sim 300$  mJy.

Fornax A is hosted by the giant early-type galaxy NGC 1316, which is the brightest member of a galaxy group at the outskirts of the Fornax cluster. NGC 1316 underwent through a major merger that likely brought large amounts of dust, cold molecular gas (Horellou et al. 2001, Galametz et al. 2014, Morokuma-Matsui et al. 2019), and neutral hydrogen (Horellou et al. 2001, Serra et al. 2019) into the centre and around the galaxy. This merger occurred  $\sim 1 - 3$  Gyr ago (e.g., Sesto et al. 2018), and it may have triggered the nuclear activity of Fornax A (e. g. McKinley et al. 2015). Nevertheless, large uncertainties remain on the timescale of formation of the radio lobes. Moreover, this past merger event does not properly explain the properties of the central emission, nor the soft X-ray cavities between the lobes and the host galaxy (Lanz et al. 2010).

The goal of this study is to measure, over a wide range of frequencies, the flux density distribution of the radio lobes and the central emission to characterise the AGN activity history that created them. For the lobes we need wide-field-of-view observations sensitive to their diffuse emission (i.e. good  $uv$ -coverage on the short baselines), while arc-second resolution is not needed. Hence, between 84 and 200 MHz we chose observations Murchison Widefield Array survey (Hurley-Walker et al. 2017). We use the MeerKAT observation to generate images of Fornax A at 1.03 (Fig. 1, left panel) and 1.44 GHz. At 1.5 GHz we chose archival Very Large Array observations (Fomalont et al. 1989). Between 5.7 and 6.9 GHz we use observations from the Sardinia Radio Telescope (Prandoni et al. 2017). Between 70 GHz and 217 GHz, we selected images from the *Planck* foreground maps (Planck Collaboration IV, 2018).

To study the central emission we selected observations with arc-second resolution (Fig. 1, right panel): the MeerKAT images at 1.03 and 1.44 GHz, archival VLA observations at 4.8 and 15 GHz (Geldzahler et al. 1984), and an observation at 108 GHz (Morokuma-Matsui et al. 2019) taken with the Atacama Large Millimeter and submillimeter Array. The left panel of Fig. 2 shows the spectral flux densities of the lobes and of the central emission we measured using these two samples. Given the morphology of the central emission, we measure its flux density by dividing it into two parts, the central unresolved

component (hereafter, the *kpc-core*) and the extended component forming the emission (the *jets*).

## 2. Spectral analysis of the main components of Fornax A

In the simplest scenario of AGN activity, the lobes (or jets) are continuously injected with particles (continuous injection model, CI). Assuming that radiative energy losses from synchrotron and inverse Compton radiation dominate over expansion losses, the radio spectrum shows a sharp cut-off whose frequency ( $\nu_{\text{break}}$ ) depends on the age of the radiation ( $t_s$ , Kardashev et al. 1962).

A more complicated scenario can be the continuous injection plus turn off model ( $\text{CI}_{\text{OFF}}$ ). The injection of high-energy particles from the nucleus starts at  $t = 0$  and at the time  $t_{\text{CI}}$  it is switched off. After that, the *off phase* of the AGN begins, and the total age of the radiation is:  $t_s = t_{\text{CI}} + t_{\text{OFF}}$  (Murgia et al. 2011). Compared to the CI model, the spectral shape is characterised by a second break-frequency ( $\nu_{\text{break, high}}$ ), beyond which the radiation spectrum drops exponentially. This frequency depends on the ratio between the dying phase ( $t_{\text{OFF}}$ ) and the total age of the source ( $\nu_{\text{break, high}} = \nu_{\text{break}}(t_s/t_{\text{OFF}})^2$ ). To determine the best-fit models of the flux density spectrum of the lobes and central emission of Fornax A, we use the software package SYNAGE++ (Murgia et al. 2011).

For both lobes, the spectral flux density shows a sharp cut-off at high frequencies (see Fig. 2, left panel). This, along with the  $\chi^2$  value of the  $\text{CI}_{\text{OFF}}$  models closer to 1 than the  $\chi^2$  of the CI models, suggests that the radio spectrum of both radio lobes is best described by the  $\text{CI}_{\text{OFF}}$  model and that currently the radio lobes are not being injected with relativistic particles.

According to the  $\text{CI}_{\text{OFF}}$  model, the dying-to-total-age ratio is  $t_{\text{OFF}}/t_s = 0.49_{-0.42}^{+0.08}$ . Assuming that the magnetic field of the lobes is  $2.6 \pm 0.3 \mu\text{G}$  (Tashiro et al. 2009), the radiative age of the east and west lobes is  $t_{s, \text{E}} = 25_{-19}^{+23}$  Myr and  $t_{s, \text{W}} = 23_{-17}^{+20}$  Myr, respectively. Likely, in the last  $t_{\text{OFF}} = 12_{-9}^{+2}$  Myr the lobes have not been replenished with relativistic particles (all parameters derived from the models are shown in Table 6 of Maccagni et al. 2020).

The spectral distribution of the *kpc-core* (in green in Fig. 2, left panel) is better described by the CI model rather than by the  $\text{CI}_{\text{OFF}}$ . The age of the synchrotron emission of the *kpc-core* is  $\sim 1_{-0.5}^{+0.3}$  Myr. By contrast, the jets are better fitted by the  $\text{CI}_{\text{OFF}}$ , and do not seem to be currently replenished with energetic particles. Their last active phase seems to have occurred  $3_{-2}^{+7}$  Myr ago and to have lasted  $\lesssim 1_{-0.5}^{+6}$  Myr.

## 3. The flickering nuclear activity of Fornax A

The properties of the flux density spectrum of the lobes of Fornax A are puzzling when compared to their projected size ( $r \sim 200$  kpc). Typically, lobes extending in the IGM for hundreds of kiloparsecs are either the remnant of an old nuclear activity, and show a steep spectrum with low break frequency, or they are currently being injected with relativistic particles, and show a jet or stream of particles connecting the AGN with the lobes. The most remarkable properties of the lobes of Fornax A are the flat spectral shape and high break frequency ( $\gtrsim 20$  GHz) of their radio emission, and that the nuclear activity that was replenishing the lobes with high-energy particles was short ( $\sim 24$  Myr) and has recently stopped ( $\sim 12$  Myr ago). The main open question therefore pertains to how these large lobes have formed in such a short time.

The right panel of Figure 2 indicates that the radiative age of the lobes of Fornax A and the dynamical age (assuming transonic expansion) are incompatible. This, along with an axial ratio of the lobes close to 1, disfavours the hypothesis that only a recent

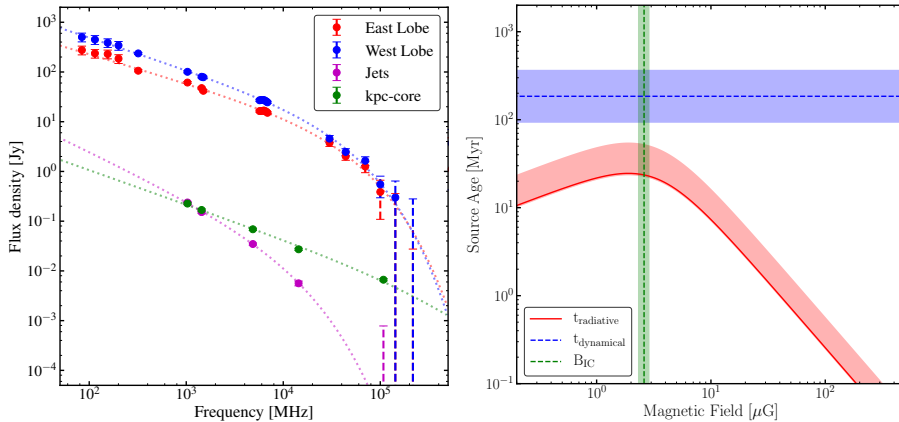


**Figure 2.** *Left panel:* Radio spectrum of the different components of Fornax A. The east lobe is shown in red, the west lobe in blue. The jets and kpc-core are in magenta and green, respectively. The dashed lines show the  $CI_{\text{OFF}}$  model of injection that best fits the flux distributions. The spectral shape of the lobes is very different from that of the inner components. *Right panel:* Comparison of radiative and dynamical age of Fornax A (red and blue shaded regions) as a function of the magnetic field. The radiative age is derived from the spectral break of the two lobes. Their magnetic field ( $B_{IC} \sim 2.6 \mu\text{G}$ ) is shown in green. (Maccagni et al. 2020)

episode of activity formed the lobes. If, instead, the lobes, filled with low-energy particles and under-pressured with respect to the surrounding IGM, were already present because of previous activities, a new nuclear phase may rapidly fill them with new high-energy particles which now dominate the radio emission of the source. This scenario would explain the overall flat radio spectrum of Fornax A and its high break-frequency. Two separate AGN outbursts have also been proposed by Lanz et al. (2010) to explain the location of the X-ray cavities relative to the radio lobes of Fornax A.

Besides the multiple activities that may have formed them, the lobes have been off for  $\sim 9$  Myr. More recently ( $\sim 3$  Myr ago) the AGN turned on again for a very short phase ( $\lesssim 1$  Myr) that formed the central jets. Given the short timescales of the different nuclear activities, Fornax A is likely rapidly flickering between an active phase and a non-active one. The recurrent activity of Fornax A may fit well in the theoretical scenario of AGN evolution whereby the central engine is active for short periods of time ( $10^4$ – $5$  years), and that these phases repeatedly occur over the total lifetime of the AGN ( $10^8$  years; e.g. Schawinski et al. 2015, Morganti et al. 2017).

After the major merger, NGC 1316 went through several accretion events and minor mergers of smaller companions (Iodice et al. 2017). These numerous interactions may have regulated the switching on and off of the multiple episodes of activity that formed the lobes as we see them now. Merger and interaction events are often invoked to explain the triggering of powerful AGNs (e. g., Ramos-Almeida et al. 2012, Sabater et al. 2013).

#### 4. Neutral and molecular gas in the centre of Fornax A

The kinematics and distribution of the cold gas in the innermost 6 kpc (Fig. 3) provide further information on the last episode of the recurrent activity of Fornax A, which generated the central jets. In the centre, ALMA observations detect  $5.6 \times 10^8 M_{\odot}$  of molecular hydrogen ( $\text{H}_2$ ) distributed in a clumpy shell around the jets (Morokuma-Matsui et al. 2019). Neutral hydrogen ( $\text{HI}$ ) clouds ( $4 \times 10^7 M_{\odot}$ ) are closely associated with the molecular gas (Serra et al. 2019). The  $\text{HI}$  seems to be more extended than the  $\text{H}_2$ , forming a halo where the molecular clouds are embedded. This is confirmed by new, yet un-

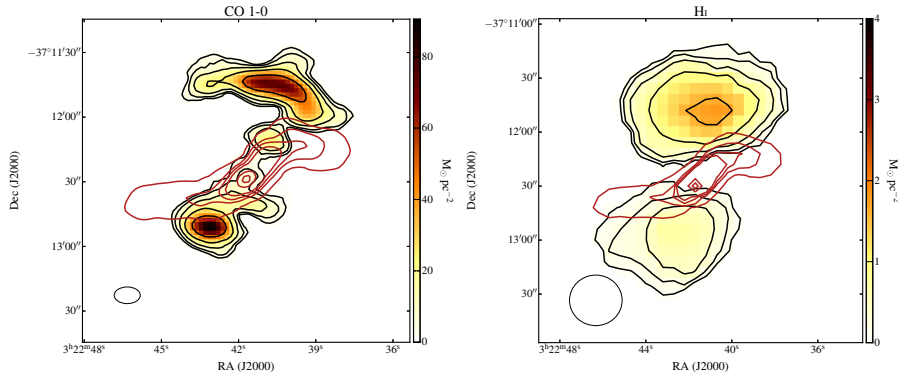


**Figure 3.** *Left panel:* Surface brightness map of the CO 1-0 line detected by ALMA (Morokuma-Matsui et al. 2019), overlaid with the radio jets. Contour levels are  $3 \times 2^n \text{ M}_\odot \text{ pc}^{-2}$ , ( $n = 0, 1, 2, \dots$ ). *Right panel:* Surface brightness map of the HI detected by MeerKAT (Serra et al. 2019), overlaid with the radio jets. Contour levels are  $0.1 \times 2^n \text{ M}_\odot \text{ pc}^{-2}$ , ( $n = 0, 1, 2, \dots$ ).

published, MeerKAT higher resolution observations which reveal a diffuse HI component surrounding the radio jets. The jets bend in the denser regions of the gas distribution (in proximity of  $\text{H}_2$  clouds with irregular kinematics) toward sparser regions (where no molecular clouds are detected but only diffuse HI, Fig. 3 right panel) suggesting a tight interplay between the nuclear activity and the surrounding cold interstellar medium.

## References

- Fabian A. C. 2012, *ARAA*, 50, 455  
 Fomalont, E. B., Ebner, K. A., van Brugel, et al. 1989, *APJ* (Letters), 346, L17  
 Galametz, M., Albrecht, M., et al. 2014, *MNRAS*, 439, 2542  
 Geldzahler, B. J., & Fomalont, E. B. 1984, *AJ*, 89, 1650  
 Harwood J. J., Hardcastle M. J., Croston J. H., et al. 2013, *MNRAS*, 435, 3353  
 Horellou, C., Black, J. H., van Gorkom, J. H., et al. 2001, *A&A*, 376, 837  
 Hurley-Walker, N., Callingham, J. R., Hancock, P. J., et al. 2017, *MNRAS*, 464, 1146  
 Iodice, E., Spavone, M., Capaccioli, M., et al. 2017, *ApJ*, 839, 21  
 Jonas, J., & MeerKAT Team 2016, *Proceedings of MeerKAT Science*, 1  
 Kardashev, N. S. 1962, *Soviet Astron.*, 6, 317  
 Kolokythas K., O’Sullivan E., Giacintucci S., et al. 2015, *MNRAS*, 450, 1732  
 Lanz, L., Jones, C., Forman, W. R., et al. 2010, *ApJ*, 721, 1702  
 Maccagni F. M., Murgia, M., Serra, P., et al. 2020, *A&A*, 634, A9  
 McKinley, B., Yang, R., López-Cañiego, M., et al. 2015, *MNRAS*, 446, 3478  
 Morganti, R. 2017, *Nature Astronomy*, 1, 596  
 Morokuma-Matsui K., Serra P., Maccagni, F. M., et al. 2019, *PASJ*, 71, 85  
 Murgia M., Fanti C., Fanti R., et al. 1999, *A&A*, 345, 769  
 Murgia M., Parma, P. Mack, H. K., et al. 2011, *A&A*, 526, A148  
 Planck Collaboration, Akrami, Y., Ashdown, M., et al. 2018, *arXiv e-prints*, arXiv:1807.06208  
 Prandoni, I., Murgia, M., Tarchi, A., et al. 2017, *A&A*, 608, A40  
 Ramos Almeida, C., Bessiere, P. S., Tadhunter, C. N., et al. 2012, *MNRAS*, 419, 687  
 Sabater, J., Best, P. N., & Argudo-Fernández, M. 2013, *MNRAS*, 430, 638  
 Schawinski, K., Koss, M., Berney, S., et al. 2015, *MNRAS*, 451, 2517  
 Serra P., Maccagni, F. M., Kleiner, D., et al. 2019, *A&A*, 628, A122  
 Sesto L. A., Faifer F. R., Smith Castelli A. V., et al. 2018, *MNRAS*, 479, 478  
 Tashiro, M. S., Isobe, N., Seta, H., et al. 2009, *PASJ*, 61, S327  
 Werner N., McNamara B. R., Churazov E., et al. 2019, *SSRv*, 215, 5